

Compressed Liquid Densities and Excess Molar Volumes of CO₂ + Hexan-1-ol Mixtures from (313 to 363) K and Pressures up to 25 MPa

Abel Zúñiga-Moreno, Luis A. Galicia-Luna,* Felix F. Betancourt-Cárdenas, and Jesús M. Bernal-García

Instituto Politécnico Nacional, ESIQIE, Laboratorio de Termodinámica, Edif. Z, Secc. 6, 1er Piso, UPALM Zacatenco, CP 07738, Lindavista, México, D.F., México

Compressed liquid densities of hexan-1-ol and of CO₂ (1) + hexan-1-ol (2) binary mixtures (at four different compositions, $x_1 = 0.1413, 0.2289, 0.3610, \text{ and } 0.6673$) have been measured from (313 to 363) K and pressures up to 25 MPa. A vibrating-tube densimeter was used to measure the experimental densities. The densities of hexan-1-ol were correlated with a short explicit volume equation and the Benedict–Webb–Rubin–Starling equation of state (BWRS EoS). Excess molar volumes were calculated using density values calculated with the BWRS EoS and the Span–Wagner EoS for hexan-1-ol and CO₂, respectively.

Introduction

Mixtures of CO₂ + alcohol are important in the chemical and biochemical industries and, for different scientific reasons, mostly connected to the development and testing of models to predict the properties of associating fluids mixed with CO₂. Supercritical fluid technology is one of the potential applications of this type of mixtures. Some of the applications of these mixtures are in reactions,¹ chromatographic separations,² and supercritical fluid extractions.³ CO₂ is widely used to extract natural products from natural resources mainly because it is inert, cheap, and recyclable. However CO₂ frequently is not capable of extracting polar substances of high molecular weight. Therefore, liquid solvents are added to increase the solvent power of supercritical CO₂.^{3,4} Additionally, these mixtures have diffusivities and viscosities that are intermediate between those of supercritical fluids and regular liquids. Thus, phase equilibria and thermophysical properties are of great significance in the development of a new process. Fluid phase equilibria has been previously reported for the system CO₂ + hexan-1-ol.^{5–12} This binary system exhibits type III phase behavior^{13,14} (based on the classification given by van Konynenburg and Scott¹³) according to the measurements reported by Nickel and Schneider,⁵ Lam et al.,⁶ Gurdial et al.,⁷ Scheidgen,⁸ Elizalde-Solis et al.,¹¹ and Beier et al.¹² On the other hand, compressed liquid densities for systems CO₂ + alcohol are scarce in the literature. The systems studied cover only mixtures containing methanol,^{15–20} ethanol,^{21,22} 1-propanol,^{23,24} and 2-propanol,^{24,25} and no experimental data were found for the system CO₂ + hexan-1-ol. In this work, densities of hexan-1-ol, and CO₂ + hexan-1-ol mixtures are measured at temperature from (313 to 363) K and pressures up to 25 MPa. Density measurements for the binary mixtures were made in single liquid phase through the whole range of temperatures and pressures measured. Densities of hexan-1-ol at high pressures have been measured previously by Bridgman,²⁶ Gylmanov et al.,²⁷ Matsuo and Makita,²⁸ Uosaki et al.,²⁹ Shakhverdiev et al.,³⁰ Garg et al.,³¹ and more recently by Audonnet and Pádua.³² Comparisons with these literature data and a published correlation for densities of hexan-1-ol³³

are made. Experimental density data are correlated using a short equation and the BWRS EoS.³⁴ The range and temperature measured here is directly related to the application of supercritical fluid technology.

Experimental Section

Materials. Hexan-1-ol (C₆H₁₄O, 102.177 g·mol⁻¹, Chemical Abstracts Service Registry No. (CASRN) 111-27-3) was from Aldrich (USA) with a stated purity of $x = 0.98$. CO₂ (44.010 g·mol⁻¹, CASRN 124-38-9) was research grade with a certified volume fraction purity of 0.99995 from Air-Products Infra (México). The reference fluids for the calibration of the vibrating-tube densimeter were water and nitrogen. Water HPLC grade was from Aldrich (USA) with a stated purity of $x = 0.9995$. Nitrogen chromatographic grade with a certified volume fraction purity of 0.99998 was from Air-Products Infra (México). Hexan-1-ol was stored over a 3 Å molecular sieve to avoid any moisture. The purities of the hexan-1-ol samples were tested using a gas chromatograph (HP 5890 series II) fitted with a flame ionization detector and a 0.9144 m × 0.003175 m diameter column packed with Chromosorb 101.¹¹ The purity after drying and distillation of hexan-1-ol was $x = 0.993$. Liquid compounds were degassed under vacuum and vigorous stirring before they were used.

Apparatus and Procedure. The apparatus and experimental procedure used in this work has been described previously.^{22,24,35} The measuring cell consisted of a vibrating-tube (Hastelloy C-276 U-tube) containing a sample of approximately 1 cm³. A visual sapphire tube cell (with a maximum volume of 12 cm³) was used to feed the measuring cell. The pressure measurements were made directly in the equilibrium cell by means of a 25 MPa Sedeme pressure transducer. The pressure transducer was thermoregulated at a specific value and calibrated periodically. The temperature was measured by three platinum probes located at the top and bottom of the sapphire cell and the over inside the vibrating tube densimeter (VTD). Temperature measurements were made in the ITS90 scale. The calibration of the vibrating-tube was performed using water and nitrogen as the reference compounds. Density reference values of water and nitrogen were obtained from the equations of state (EoS) proposed by Wagner and Pruss³⁶ and Span et al.,³⁷ respectively.

* Corresponding author. E-mail: lgalicial@ipn.mx. Phone: +52 55-5729-6000, ext 55133. Fax: +52 55-5586-2728.

Table 1. Density (ρ) for Hexan-1-ol at Six Temperatures

$T/K = 313.14$		$T/K = 323.12$		$T/K = 333.01$		$T/K = 342.96$		$T/K = 352.86$		$T/K = 362.80$	
P/MPa	$\rho/\text{kg}\cdot\text{m}^{-3}$	P/MPa	$\rho/\text{kg}\cdot\text{m}^{-3}$	P/MPa	$\rho/\text{kg}\cdot\text{m}^{-3}$	P/MPa	$\rho/\text{kg}\cdot\text{m}^{-3}$	P/MPa	$\rho/\text{kg}\cdot\text{m}^{-3}$	P/MPa	$\rho/\text{kg}\cdot\text{m}^{-3}$
1.034	804.9	1.021	797.6	1.023	790.2	1.036	782.9	1.020	775.0	1.011	767.0
2.032	805.6	2.009	798.4	2.011	791.0	2.011	783.7	2.012	775.9	2.009	768.0
3.046	806.3	3.003	799.1	3.042	791.8	3.012	784.5	3.028	776.9	3.024	769.0
4.016	807.0	4.014	799.8	4.000	792.6	4.015	785.4	4.014	777.7	4.006	769.9
5.013	807.7	5.025	800.6	5.014	793.3	5.007	786.2	5.010	778.6	5.021	770.8
6.035	808.4	6.021	801.3	6.004	794.1	6.013	787.0	6.028	779.5	6.035	771.8
7.010	809.1	7.032	802.1	7.021	794.9	7.039	787.8	7.039	780.4	7.009	772.6
8.036	809.8	8.016	802.8	8.012	795.7	8.023	788.6	8.000	781.2	8.023	773.6
9.015	810.5	9.016	803.5	9.002	796.4	9.022	789.4	9.030	782.1	9.041	774.5
10.002	811.2	10.019	804.2	10.004	797.2	10.035	790.2	10.033	782.9	10.000	775.3
11.020	811.8	11.015	805.0	11.026	797.9	11.017	791.0	11.014	783.7	11.014	776.2
12.017	812.5	12.012	805.7	12.020	798.7	12.017	791.7	12.017	784.5	12.026	777.1
13.002	813.2	13.015	806.3	13.018	799.4	13.023	792.5	13.014	785.3	13.045	777.9
14.016	813.8	14.006	807.0	14.009	800.1	14.003	793.2	14.011	786.1	14.030	778.8
15.016	814.5	15.002	807.7	15.019	800.8	15.009	793.9	15.010	786.9	15.012	779.6
16.009	815.1	16.013	808.4	16.017	801.6	16.014	794.7	16.023	787.7	16.031	780.4
17.010	815.8	17.016	809.1	17.006	802.3	17.038	795.4	17.018	788.5	17.003	781.2
18.010	816.4	18.018	809.7	18.018	803.0	18.023	796.1	18.016	789.3	18.020	782.0
19.012	817.1	19.000	810.4	19.013	803.7	19.015	796.8	19.014	790.0	19.033	782.8
20.019	817.7	20.003	811.0	20.037	804.4	20.015	797.5	20.021	790.8	20.004	783.6
21.006	818.3	21.009	811.7	21.029	805.0	21.026	798.1	21.017	791.5	21.006	784.4
22.037	818.9	22.000	812.3	22.008	805.7	22.003	798.8	22.038	792.3	22.032	785.2
23.037	819.6	23.002	813.0	23.026	806.4	23.005	799.5	23.016	793.0	22.989	785.9
24.010	820.2	24.021	813.6	24.019	807.0	24.003	800.1	24.020	793.7	24.055	786.7
25.023	820.8	25.004	814.3	25.025	807.7	25.031	800.8	25.048	794.5	25.035	787.5

Details about the calibrating procedures of the platinum temperature probes, the pressure transducer, and the vibrating-tube densimeter have been given in previous papers.^{22,35,38} The uncertainties of the experimental quantities presented in this work are estimated to be $T/K = \pm 0.03$, $P/\text{MPa} = \pm 0.008$, and $\rho/\text{kg}\cdot\text{m}^{-3} = \pm 0.2$ for liquid density in the range of the reported data, in a similar mode as preceding reported data.^{39,40}

Loading of the Measurement Cell. A detailed procedure of loading the measurement cell has been presented in preceding papers.^{22,24} The samples with the desired compositions were prepared by successive loadings of a known mass¹⁶ of the pure compounds in the sapphire feeding cell. The amounts of the pure compounds were determined by weighting carried out with an uncertainty of $\pm 10^{-7}$ kg with a Sartorius comparator balance (MCA1200), which was periodically calibrated with a standard mass of 1 kg class E1. The resulting uncertainty for the mole fraction composition of the mixtures was lower than $\pm 10^{-4}$.

Theory. A short explicit volume equation of six parameters⁴¹ was used to correlate the densities reported herein. This equation is expressed as follows:

$$v = \frac{d_1 + d_2P}{d_3 - d_4T + d_5T^{1/2} + d_6P} \quad (1)$$

where v is the specific volume, and d_i are adjustable parameters. The BWRS EoS³⁴ was also used to correlate the experimental densities. This EoS can be written as

$$P = \frac{RT}{V_m} + \frac{(B_0RT - A_0 - C_0/T^2 + D_0/T^3 - E_0/T^4)}{V_m^2} + \frac{(bRT - a - d/T)}{V_m^3} + \frac{\alpha(a + d/T)}{V_m^6} + \frac{c(1 + u/V_m^2) \exp(-u/V_m^2)}{V_m^3 T^2} \quad (2)$$

where V_m is the molar volume. A Marquardt–Levenberg least-squares optimization procedure^{22,35} is used to fit the parameters in eq 1 and eq 2 using the following objective function, S :

$$S = \sum_{i=1}^n \left[\frac{\rho_i^{\text{exp}} - \rho_i^{\text{cal}}}{\rho_i^{\text{exp}}} \right]^2 \quad (3)$$

where n is the number of experimental data points, and the superscripts exp and cal represent the experimental density and the value obtained from the model, respectively. The average absolute deviation (AAD), the mean deviation (bias), the standard deviation (SDV), and the root mean square (RMS) are used to evaluate the different correlations. These statistical values were used according to the definitions given in former papers.^{39–41}

Results and Discussion

Densities were determined for hexan-1-ol and four different compositions for the system CO_2 + hexan-1-ol. Measurements were carried out along six isotherms, from (1 to 25) MPa. The experimental results are shown in Table 1 through Table 5. The reported values of density were correlated using eq 1 and eq 2. The correlation of the mixture data was made at constant composition for each set of data. Parameters along with statistical values for the correlations of hexan-1-ol and the four different compositions of the system CO_2 + hexan-1-ol are reported in Table 6. Relative deviations of experimental data (ρ^{exp}) and values calculated with the two correlations (ρ^{cal}) using the adjusted parameters reported in Table 6 for hexan-1-ol are shown in Figure 1. The maximum deviations are ± 0.03 % for the six-parameter equation, and the standard deviation reported in Table 6 is 0.01 %. These values suggest that this equation represents the experimental data within the experimental uncertainty. Similar results were obtained for the BWRS EoS as can be seen from Figure 1 and the standard deviation reported in Table 6; therefore, both correlations are capable to represent the experimental data within the experimental uncertainty.

To check for the consistency of the experimental densities of hexan-1-ol, comparisons with published density data were made. Comparisons with literature data and values calculated with the two correlations were performed in the same range of temperature and pressure reported here; however, only relative deviations of density data sets from literature (ρ^{lit}) and values calculated with the BWRS EoS (ρ^{cal}) using the adjusted parameters reported in Table 6 are plotted in Figure 2. The maximum relative deviations observed were of -0.3 %, ± 0.05 %, $+0.55$ %, ± 0.1 %, and ± 0.2 % for the data reported by Gylmanov et al.,²⁷ Matsuo and Makita,²⁸ Shakverdiev et al.,³⁰ Garg et al.,³¹ and Audonnet and Pádua,³² respectively. Similar

Table 2. Density (ρ) and Excess Molar Volumes (V_m^E) for CO₂ (1) + Hexan-1-ol (2)

P/MPa	$\rho/\text{kg}\cdot\text{m}^{-3}$	$V_m^E/\text{cm}^3\cdot\text{mol}^{-1}$	P/MPa	$\rho/\text{kg}\cdot\text{m}^{-3}$	$V_m^E/\text{cm}^3\cdot\text{mol}^{-1}$	P/MPa	$\rho/\text{kg}\cdot\text{m}^{-3}$	$V_m^E/\text{cm}^3\cdot\text{mol}^{-1}$
			$x_1 = 0.1413$					
$T/\text{K} = 313.13$			$T/\text{K} = 323.10$			$T/\text{K} = 332.65$		
8.001	814.4	-15.3	8.003	806.8	-21.2	8.012	799.2	-24.9
9.030	815.2	-5.6	9.008	807.6	-14.6	9.010	800.1	-18.9
10.001	816.0	-2.9	10.001	808.4	-9.0	9.940	801.0	-14.2
11.001	816.7	-2.1	11.000	809.2	-5.2	11.006	801.8	-9.9
12.003	817.5	-1.7	12.000	810.0	-3.5	12.012	802.6	-6.8
12.999	818.2	-1.4	12.999	810.8	-2.7	12.998	803.5	-4.9
13.988	818.9	-1.2	14.000	811.5	-2.2	14.006	804.3	-3.8
15.000	819.6	-1.1	15.002	812.3	-1.8	14.996	805.1	-3.0
15.998	820.4	-0.9	16.000	813.0	-1.6	16.003	805.9	-2.5
16.988	821.1	-0.8	16.997	813.7	-1.4	17.010	806.7	-2.2
17.997	821.7	-0.7	18.008	814.5	-1.2	18.025	807.5	-1.9
19.003	822.5	-0.6	19.006	815.2	-1.1	19.008	808.2	-1.6
20.002	823.1	-0.6	20.026	816.0	-0.9	19.999	809.0	-1.5
20.995	823.8	-0.5	21.007	816.7	-0.8	21.015	809.7	-1.3
22.009	824.5	-0.4	22.022	817.4	-0.8	21.988	810.5	-1.2
22.957	825.1	-0.4	23.003	818.1	-0.7	23.000	811.2	-1.0
24.000	825.8	-0.3	24.000	818.8	-0.6	24.025	812.0	-0.9
$T/\text{K} = 342.99$			$T/\text{K} = 352.87$			$T/\text{K} = 362.75$		
8.000	791.4	-28.3	8.000	783.3	-31.1	8.000	774.2	-33.4
9.011	792.3	-22.4	9.011	784.2	-25.1	9.015	775.2	-27.4
10.009	793.2	-17.6	10.009	785.2	-20.4	10.008	776.3	-22.6
11.008	794.0	-13.7	11.002	786.1	-16.5	11.003	777.2	-18.8
12.009	794.9	-10.5	12.012	787.0	-13.3	12.009	778.2	-15.5
13.021	795.7	-8.0	13.023	788.0	-10.7	12.997	779.2	-12.9
14.029	796.6	-6.2	14.009	788.9	-8.7	14.006	780.1	-10.7
15.034	797.4	-4.9	15.002	789.8	-7.0	15.014	781.0	-8.9
16.012	798.2	-4.0	16.008	790.6	-5.8	16.007	781.9	-7.4
17.004	799.0	-3.4	17.006	791.5	-4.8	17.010	782.9	-6.3
18.009	799.8	-2.9	18.009	792.4	-4.1	18.025	783.9	-5.3
19.012	800.5	-2.5	18.999	793.2	-3.5	19.041	784.7	-4.5
19.994	801.3	-2.2	19.979	794.0	-3.1	20.017	785.6	-4.0
21.005	802.1	-1.9	21.018	794.8	-2.7	21.025	786.5	-3.5
22.011	802.9	-1.7	22.009	795.7	-2.4	22.013	787.3	-3.1
22.994	803.6	-1.5	23.005	796.5	-2.2	23.010	788.2	-2.7
24.019	804.3	-1.4	24.001	797.3	-2.0	24.019	789.1	-2.4

results can be obtained for the six-parameter equation. Excellent agreement was observed with the data reported by Matsuo and Makita.²⁸ The data reported by Garg et al.³¹ were in good agreement with the density values calculated with the BWRS EoS; for the remaining sets of data, the deviations were larger as it is depicted in Figure 2.

The extrapolation of densities at atmospheric pressure using the BWRS EoS was also tested. Density values calculated at atmospheric pressure for hexan-1-ol with the BWRS EoS (ρ^{cal}) are compared with published data^{28,31,42-48} (ρ^{lit}). The relative deviations are $\pm 0.1\%$ for all data as can be seen in Figure 3, having a better agreement with the data reported by Rodriguez et al.,⁴⁶ Hoyuelos et al.,⁴⁷ and most of the data reported by Matsuo and Makita.²⁸

Comparison of our experimental data of hexan-1-ol with the correlation reported by Cibulka and Zikova³³ is illustrated in Figure 4. The maximum deviations are $+0.01\%$ and -0.06% , although to evaluate this comparison the $\text{RMSD}/\text{kg}\cdot\text{m}^{-3}$, $\text{RMSD}_r/\%$, and $\text{bias}/\text{kg}\cdot\text{m}^{-3}$ as defined by Cibulka and Zikova³³ were calculated for our set of data. The results are as follows: $0.17\text{ kg}\cdot\text{m}^{-3}$, 0.02% , and $-0.13\text{ kg}\cdot\text{m}^{-3}$, respectively. The RMSD and RMSD_r values are slightly higher than those obtained for the data of Matsuo and Makita²⁸ and Garg et al.³¹ (see ref 33). The good agreement with these two data sets is therefore confirmed.

The excess volumes were calculated in the whole temperature and pressure intervals according to the relation:

$$V_m^E = \frac{x_1 W_1 + x_2 W_2}{\rho^{\text{mix}}} - (x_1 V_{m1} + x_2 V_{m2}) \quad (4)$$

where V_m^E is the molar excess volume; ρ^{mix} is the density of the

mixture; V_{m1} and V_{m2} are the pure component molar volumes at the measured temperature and pressure of the mixture; W_1 and W_2 are the molecular weights; and x_1 and x_2 are the mole fractions of CO₂ and hexan-1-ol, respectively. Densities of hexan-1-ol were calculated in the reported range of pressure and temperature by using the BWRS EoS with the adjusted parameters reported in Table 6. The molar volumes of CO₂ were obtained using the equation of state proposed by Span and Wagner.⁴⁹ The uncertainty in the excess molar volumes is estimated to be $\pm 0.15\%$, as previously reported.⁴⁰ A typical behavior of the excess molar volumes as function of pressure for this type of mixture is shown in Figure 5. The excess molar volumes become less negative as the pressure is increased at constant temperature; on the other hand, the excess molar volumes become more negative as the temperature is increased at constant pressure, as illustrated in Figure 5. Although only the composition at $x_1 = 0.2289$ is depicted in Figure 5, the same behavior is obtained for all the compositions studied in this work.

Treszczanowicz et al.⁵⁰ suggested that V_m^E is the result of different opposing effects, divided in chemical, physical, and structural contributions. Physical contributions, which are nonspecific interactions between real species present in the mixtures, contribute a positive term to V_m^E . The chemical interactions effects contribute to negative values of V_m^E ; these interactions include dipole-dipole interactions. The structural contributions arise specially from interstitial accommodation; this effect contributes to negative values of V_m^E . Nickel and Schneider⁵ performed near-infrared spectroscopic studies on the phase behavior of hexan-1-ol in CO₂. These studies allowed the determination of the alcohol concentration and of nonas-

Table 3. Density (ρ) and Excess Molar Volumes (V_m^E) for CO₂ (1) + Hexan-1-ol (2)

P/MPa	$\rho/\text{kg}\cdot\text{m}^{-3}$	$V_m^E/\text{cm}^3\cdot\text{mol}^{-1}$	P/MPa	$\rho/\text{kg}\cdot\text{m}^{-3}$	$V_m^E/\text{cm}^3\cdot\text{mol}^{-1}$	P/MPa	$\rho/\text{kg}\cdot\text{m}^{-3}$	$V_m^E/\text{cm}^3\cdot\text{mol}^{-1}$
			$x_1 = 0.2289$					
			$T/\text{K} = 323.09$			$T/\text{K} = 332.66$		
6.000	817.2	-56.2	8.001	810.9	-34.5	8.001	802.7	-40.6
7.000	818.0	-39.6	9.023	811.8	-23.7	9.021	803.7	-30.6
8.000	818.8	-25.0	10.003	812.7	-14.7	10.005	804.6	-22.7
9.007	819.7	-9.4	11.001	813.5	-8.6	10.998	805.6	-16.2
10.003	820.5	-4.8	12.000	814.4	-5.9	12.010	806.5	-11.3
11.000	821.3	-3.6	12.993	815.2	-4.5	12.988	807.4	-8.2
12.000	822.1	-2.9	14.005	816.0	-3.7	14.031	808.2	-6.2
13.000	822.9	-2.5	15.003	816.9	-3.1	14.998	809.1	-5.1
14.000	823.7	-2.1	15.998	817.7	-2.7	15.995	810.0	-4.2
15.002	824.5	-1.9	17.001	818.5	-2.4	17.006	810.9	-3.6
15.997	825.2	-1.7	18.010	819.3	-2.1	18.026	811.7	-3.2
17.001	826.0	-1.5	19.003	820.1	-1.9	18.999	812.5	-2.8
18.004	826.8	-1.3	20.023	820.9	-1.7	19.994	813.3	-2.5
19.000	827.5	-1.2	20.983	821.6	-1.6	21.009	814.1	-2.3
20.022	828.3	-1.1	22.021	822.4	-1.4	21.988	814.9	-2.1
20.989	829.0	-1.0	23.004	823.1	-1.3	22.998	815.8	-1.9
22.004	829.7	-0.9	24.003	824.0	-1.2	24.033	816.6	-1.7
23.004	830.4	-0.8						
24.002	831.2	-0.7						
			$T/\text{K} = 342.15$			$T/\text{K} = 352.88$		
7.999	794.5	-45.5	7.999	785.4	-50.4	7.999	775.8	-54.3
9.012	795.5	-35.8	9.001	786.5	-40.8	9.002	776.9	-44.5
10.003	796.5	-28.2	10.003	787.5	-33.1	10.005	778.1	-36.8
10.998	797.4	-21.9	11.003	788.6	-26.9	10.998	779.2	-30.5
12.004	798.4	-16.7	12.008	789.6	-21.7	12.004	780.3	-25.3
13.005	799.3	-12.7	13.016	790.6	-17.5	13.018	781.4	-20.9
14.031	800.2	-9.8	14.015	791.6	-14.1	14.013	782.4	-17.4
15.032	801.2	-7.8	14.991	792.6	-11.5	15.005	783.5	-14.5
15.995	802.0	-6.4	16.001	793.6	-9.5	16.000	784.5	-12.2
17.010	802.9	-5.4	16.996	794.5	-7.9	17.004	785.5	-10.3
18.015	803.8	-4.6	18.009	795.5	-6.7	18.020	786.5	-8.8
18.999	804.6	-4.0	19.001	796.4	-5.8	18.993	787.5	-7.6
19.994	805.5	-3.5	19.982	797.3	-5.1	19.987	788.5	-6.6
21.000	806.3	-3.1	21.013	798.3	-4.5	21.029	789.5	-5.8
21.898	807.1	-2.9	21.910	799.0	-4.1	21.917	790.3	-5.2
23.030	808.0	-2.5	23.005	800.0	-3.6	22.966	791.3	-4.6
24.008	808.8	-2.3	24.002	800.9	-3.3	23.998	792.3	-4.2

Table 4. Density (ρ) and Excess Molar Volumes (V_m^E) for CO₂ (1) + Hexan-1-ol (2)

P/MPa	$\rho/\text{kg}\cdot\text{m}^{-3}$	$V_m^E/\text{cm}^3\cdot\text{mol}^{-1}$	P/MPa	$\rho/\text{kg}\cdot\text{m}^{-3}$	$V_m^E/\text{cm}^3\cdot\text{mol}^{-1}$	P/MPa	$\rho/\text{kg}\cdot\text{m}^{-3}$	$V_m^E/\text{cm}^3\cdot\text{mol}^{-1}$
			$x_1 = 0.3610$					
			$T/\text{K} = 323.02$			$T/\text{K} = 332.95$		
8.000	825.3	-39.3	8.000	816.1	-54.2	8.000	806.7	-64.1
9.000	826.3	-14.8	9.000	817.0	-37.4	9.000	807.6	-48.8
10.001	827.3	-7.6	10.001	818.1	-23.1	10.001	808.8	-36.1
11.000	828.3	-5.6	11.000	819.1	-13.4	11.000	809.9	-25.8
12.000	829.2	-4.6	12.000	820.1	-9.1	12.000	811.0	-18.0
13.000	830.2	-3.9	13.000	821.1	-7.0	13.000	812.1	-13.0
14.001	831.0	-3.3	14.001	822.1	-5.7	14.001	813.1	-9.9
15.000	832.0	-2.9	15.000	823.1	-4.9	15.000	814.1	-8.0
16.000	832.9	-2.6	16.000	824.0	-4.2	16.000	815.1	-6.7
17.001	833.8	-2.3	17.001	824.9	-3.7	17.001	816.1	-5.8
18.000	834.6	-2.1	18.000	825.9	-3.3	18.000	817.1	-5.0
19.000	835.5	-1.9	19.000	826.8	-3.0	19.000	818.1	-4.4
20.000	836.3	-1.7	20.000	827.7	-2.7	20.000	819.1	-4.0
21.000	837.2	-1.5	21.000	828.6	-2.4	21.000	820.0	-3.6
22.000	838.1	-1.4	22.000	829.5	-2.2	22.000	820.9	-3.2
23.004	838.9	-1.3	23.004	830.4	-2.0	23.004	821.9	-2.9
24.000	839.7	-1.1	24.000	831.3	-1.8	24.000	822.8	-2.7
			$T/\text{K} = 342.80$			$T/\text{K} = 352.72$		
8.000	797.5	-72.2	8.000	787.3	-79.2	8.000	776.7	-85.5
9.000	798.3	-57.1	9.000	788.6	-64.1	9.000	777.5	-70.1
10.001	799.5	-44.9	10.001	789.9	-52.0	10.001	778.9	-57.9
11.000	800.6	-35.0	11.000	791.1	-42.1	11.000	780.4	-48.0
12.000	801.8	-26.9	12.000	792.3	-34.0	12.000	781.7	-39.8
13.000	802.9	-20.5	13.000	793.5	-27.4	13.000	783.0	-33.0
14.001	804.0	-15.9	14.001	794.7	-22.1	14.001	784.3	-27.4
15.000	805.0	-12.6	15.000	795.9	-17.9	15.000	785.6	-22.8
16.000	806.1	-10.3	16.000	797.0	-14.7	16.000	786.7	-19.1
17.001	807.1	-8.6	17.001	798.2	-12.3	17.001	788.0	-16.1
18.000	808.1	-7.4	18.000	799.3	-10.5	18.000	789.2	-13.8
19.000	809.1	-6.4	19.000	800.4	-9.0	19.000	790.3	-11.9
20.000	810.2	-5.7	20.000	801.5	-7.9	20.000	791.5	-10.3
21.000	811.1	-5.0	21.000	802.5	-7.0	21.000	792.7	-9.1
22.000	812.1	-4.5	22.000	803.6	-6.2	22.000	793.8	-8.1
23.004	813.1	-4.1	23.004	804.7	-5.6	23.004	794.9	-7.2
24.000	814.0	-3.7	24.000	805.7	-5.1	24.000	796.0	-6.5

sociated molecules; therefore, it is possible to get information about the association behavior. They found that the total mass

concentration of hexan-1-ol in the liquid phase of the system CO₂ + hexan-1-ol is formed by a monomeric alcohol and

Table 5. Density (ρ) and Excess Molar Volumes (V_m^E) for CO₂ (1) + Hexan-1-ol (2)

P/MPa	$\rho/\text{kg}\cdot\text{m}^{-3}$	$V_m^E/\text{cm}^3\cdot\text{mol}^{-1}$	P/MPa	$\rho/\text{kg}\cdot\text{m}^{-3}$	$V_m^E/\text{cm}^3\cdot\text{mol}^{-1}$	P/MPa	$\rho/\text{kg}\cdot\text{m}^{-3}$	$V_m^E/\text{cm}^3\cdot\text{mol}^{-1}$
$T/\text{K} = 313.12$			$x_1 = 0.6673$ $T/\text{K} = 323.04$			$T/\text{K} = 332.91$		
10.006	832.2	-12.0						
11.070	839.5	-8.9						
11.984	844.0	-7.5	11.958	805.1	-13.8			
12.978	847.7	-6.5	13.000	820.5	-11.0			
14.001	851.0	-5.7	14.003	827.7	-9.2	13.994	792.4	-14.7
15.000	854.0	-5.1	14.985	832.2	-7.9	15.014	802.9	-11.9
16.000	856.8	-4.6	15.989	836.1	-6.9	16.021	811.3	-10.2
17.001	859.5	-4.2	16.987	839.5	-6.1	16.986	816.5	-8.9
18.000	862.1	-3.9	17.900	842.4	-5.6	17.972	820.9	-7.8
19.000	864.4	-3.6	19.002	845.6	-5.0	18.945	824.7	-7.0
20.000	866.8	-3.4	20.011	848.3	-4.6	19.945	828.5	-6.3
21.000	869.0	-3.2	21.004	850.9	-4.3	20.986	832.0	-5.8
22.000	871.2	-3.0	22.004	853.4	-4.0	21.983	835.1	-5.3
23.004	873.2	-2.8	22.970	855.7	-3.7	22.933	838.0	-4.9
24.000	875.2	-2.7	24.005	857.8	-3.5	24.057	841.0	-4.5
$T/\text{K} = 342.84$			$T/\text{K} = 352.76$			$T/\text{K} = 362.63$		
16.026	783.0	-15.1						
17.179	792.3	-12.4						
18.132	798.6	-10.8	17.936	777.4	-16.0	18.009	753.1	-20.6
19.020	803.4	-9.7	19.013	785.2	-13.7	18.957	764.4	-18.4
20.034	808.1	-8.6	20.014	790.9	-12.1	20.037	772.1	-16.0
20.962	811.8	-7.7	20.987	795.3	-10.7	21.016	777.3	-14.1
21.983	815.6	-7.0	22.012	799.8	-9.6	22.000	781.8	-12.6
22.865	818.7	-6.5	22.999	803.6	-8.7			
23.906	822.1	-5.9	23.951	806.9	-8.0			

Table 6. Temperature, Pressure and Density Range, Data Points (n), and Parameters for the Two Correlation Models for Hexan-1-ol, and CO₂ (1) + Hexan-1-ol (2) Mixtures and Statistical Values^a

	hexan-1-ol	$x_1 = 0.1413$	$x_1 = 0.2289$	$x_1 = 0.3610$	$x_1 = 0.6673$
T_{\min}/K	313.14	313.13	313.13	313.09	312.88
T_{\max}/K	362.80	362.75	362.60	362.56	362.63
P_{\min}/MPa	1.011	8.000	6.000	8.000	10.006
P_{\max}/MPa	25.048	24.025	24.033	24.000	24.057
$\rho_{\min}/\text{kg}\cdot\text{m}^{-3}$	767.0	774.1	775.7	767.6	753.0
$\rho_{\max}/\text{kg}\cdot\text{m}^{-3}$	820.8	825.8	831.1	839.7	875.2
n	150	102	104	102	60
Six-Parameters					
$d_1/\text{MPa}\cdot\text{m}^3\cdot\text{kg}^{-1}$	-6.540	-157.485	-223.356	-169.183	6.948
$d_2/\text{m}^3\cdot\text{kg}^{-1}$	-0.03634	-0.95696	-1.57836	-1.3524	-8.39012
d_3/MPa	-4679.4	-59781.5	-85929.5	-60648.5	-61865.0
$d_4/\text{MPa}\cdot\text{K}^{-1}$	-11.320	-455.935	-676.759	-571.059	-390.483
$d_5/\text{MPa}\cdot\text{K}^{-1/2}$	-233.03	-11879.17	-17364.78	-14486.62	-2756.01
d_6	-34.16	-906.95	-1491.97	-1295.01	-7555.33
AAD/%	0.01	0.02	0.02	0.02	0.16
bias/%	0.0005	0.0001	0.0001	-0.0002	0.0003
SDV/%	0.01	0.03	0.03	0.03	0.20
RMS/%	0.01	0.03	0.03	0.03	0.20
BWRS EoS					
$B_0/\text{cm}^3\cdot\text{mol}^{-1}$	398.92	422.89	2611.20	1802.66	1429.46
$A_0/\text{bar}\cdot\text{cm}^6\cdot\text{mol}^{-2}$	3.7753×10^7	2.8936×10^7	8.6772×10^7	6.7722×10^7	3.6073×10^7
$C_0/\text{bar}\cdot\text{K}^2\cdot\text{cm}^6\cdot\text{mol}^{-2}$	1.2543×10^{12}	3.1228×10^{12}	5.5687×10^{11}	5.9561×10^{11}	-6.4697×10^{11}
$D_0/\text{bar}\cdot\text{K}^3\cdot\text{cm}^6\cdot\text{mol}^{-2}$	-3.2235×10^{14}	-3.8227×10^{14}	1.1752×10^{15}	1.2141×10^{15}	9.3667×10^{14}
$E_0/\text{bar}\cdot\text{K}^4\cdot\text{cm}^6\cdot\text{mol}^{-2}$	-1.3798×10^{17}	-2.6354×10^{17}	2.0812×10^{17}	2.2789×10^{17}	2.0680×10^{17}
$b/\text{cm}^6\cdot\text{mol}^{-2}$	4.8698×10^4	3.9033×10^3	-1.1583×10^5	-4.3040×10^4	-7.7136×10^4
$a/\text{bar}\cdot\text{cm}^9\cdot\text{mol}^{-3}$	3.2074×10^8	4.4107×10^8	5.3592×10^8	5.1981×10^8	3.3373×10^8
$d/\text{bar}\cdot\text{K}\cdot\text{cm}^9\cdot\text{mol}^{-3}$	4.2905×10^{10}	-6.5417×10^{10}	-3.8760×10^{10}	-2.1404×10^{10}	-7.1862×10^{10}
$c/\text{bar}\cdot\text{K}^2\cdot\text{cm}^9\cdot\text{mol}^{-3}$	-2.9969×10^{14}	1.1808×10^{15}	1.1808×10^{15}	1.1808×10^{15}	1.1808×10^{15}
$\alpha/\text{cm}^9\cdot\text{mol}^{-3}$	2.6655×10^7	2.6019×10^7	1.2634×10^7	5.2279×10^6	3.0940×10^6
$u/\text{cm}^6\cdot\text{mol}^{-2}$	1.1509×10^4	3.8643×10^7	3.8643×10^7	3.8643×10^7	3.8643×10^7
AAD/%	0.01	0.03	0.02	0.02	0.23
bias/%	-0.0006	-0.0002	-0.0003	-0.0002	0.0006
SDV/%	0.01	0.04	0.02	0.02	0.29
RMS/%	0.01	0.04	0.02	0.02	0.29

^a AAD, average absolute deviation; bias, mean deviation; SDV, standard deviation; and RMS, root mean square.

associated alcohol species. From the results obtained, Nickel and Schneider⁵ conclude that in the liquid region most of the alcohol is associated at low temperatures but the mass concentration of monomer increased as the temperature increases. Although the effect is less pronounced, the mass concentration

of monomer decreased as the pressure was increased at constant temperature, as can be demonstrated with the data reported in Table 3 in the work by Nickel and Schneider.⁵ Based on the discussion of Treszczanowicz et al.,⁵⁰ the results given by Nickel and Schneider,⁵ and the behavior of the excess molar volume

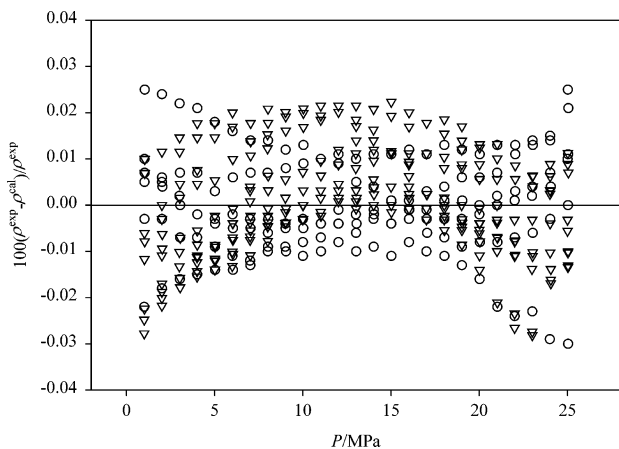


Figure 1. Relative deviations of experimental densities reported here (ρ^{exp}) and values calculated (ρ^{cal}) with the two correlations used in this work, using the adjusted parameters reported in Table 6 for hexan-1-ol: \circ , six-parameter equation; ∇ , BWRs EoS.

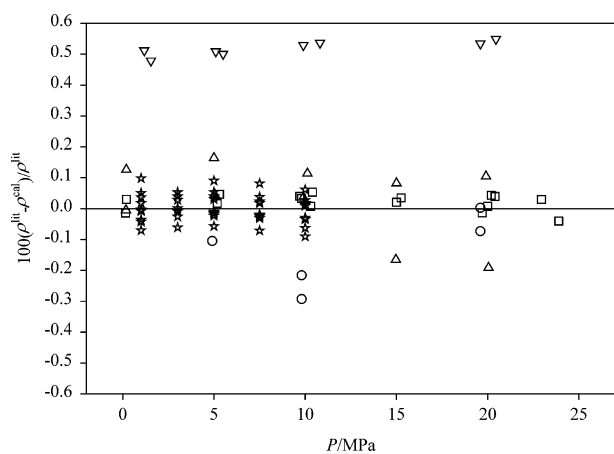


Figure 2. Relative deviations of experimental densities from literature (ρ^{exp}) and values calculated (ρ^{cal}) with the BWRs EoS using the parameters reported in Table 6 for hexan-1-ol: \circ , ref 27; \square , ref 28; ∇ , ref 30; \star , ref 31; \triangle , ref 32.

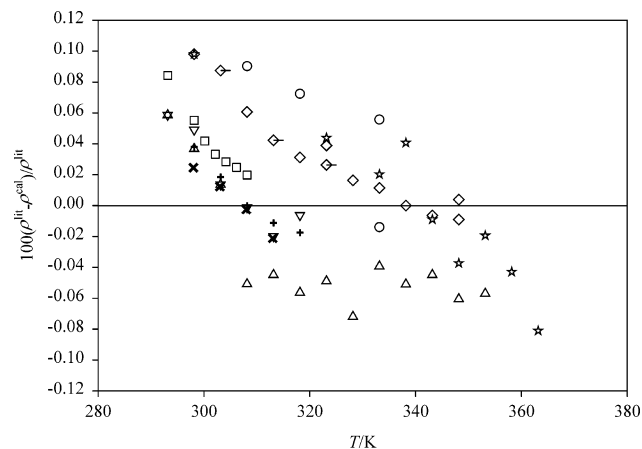


Figure 3. Relative deviations of experimental densities at atmospheric pressure for hexan-1-ol from literature (ρ^{exp}) and values calculated (ρ^{cal}) with the BWRs EoS using the parameters reported in Table 6: \circ , ref 42; ∇ , ref 43; \square , ref 44; \diamond , ref 28; \triangle , ref 45; \star , ref 31; \times , ref 46; $+$, ref 47; $-$, ref 48.

of the $\text{CO}_2 + \text{hexan-1-ol}$, the interactions in this system are described as follows. Nickel and Schneider⁵ shown that in the low-temperature region most of the molecules of alcohol are associated, then the interactions with the CO_2 molecules are weak, resulting in small negative values for the excess molar

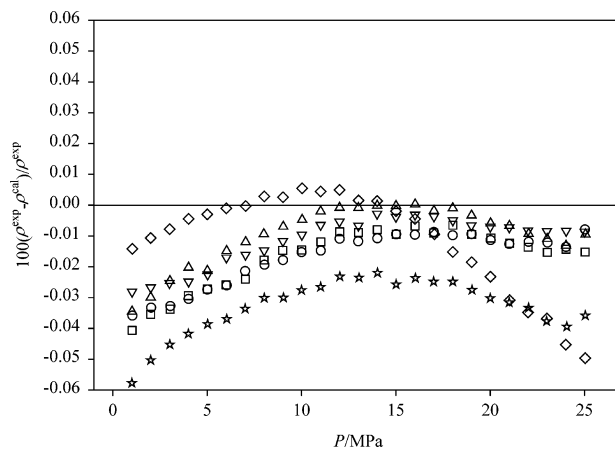


Figure 4. Relative deviations of experimental densities from this work (ρ^{exp}) and those values calculated (ρ^{cal}) with the correlation reported by Cibulka and Zikova³³ for hexan-1-ol at the following temperatures: \circ , 313.14 K; ∇ , 323.12 K; \square , 333.01 K; \diamond , 342.96 K; \triangle , 352.86 K; \star , 362.80 K.

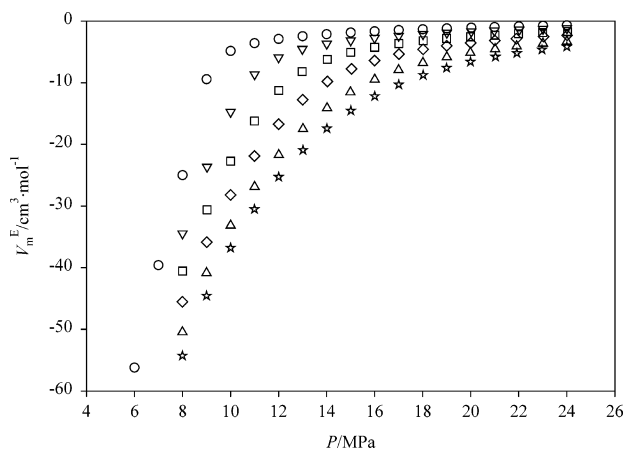


Figure 5. Excess molar volumes as function of pressure for the mixture CO_2 (1) + hexan-1-ol (2), $x_1 = 0.2289$ at \circ , 313.13 K; ∇ , 323.09 K; \square , 332.66 K; \diamond , 342.15 K; \triangle , 352.88 K; \star , 362.60 K.

volume. As the temperature is increased, the hydrogen bond interaction starts to break and the interaction between the monomeric alcohol molecules and CO_2 increase, these will result on greater negative values for the excess molar volume. At constant temperature, when the pressure increased the number of monomer molecules of alcohol decrease⁵ and the interaction between alcohol and CO_2 molecules becomes weak, then the molar volume becomes closer to the mixture ideal volume.

Conclusions

Densities of pure hexan-1-ol and $\text{CO}_2 + \text{hexan-1-ol}$ binary mixtures at four different mole fractions were studied as a function of temperature and pressure. Densities of hexan-1-ol were in good agreement with published data. For the range of temperature and pressures studied here, the six-parameter model presents similar deviations than those obtained from the BWRs EoS. The six-parameter model is more practical to use in engineering due to less parameters and being volume explicit. Thus, it can be easily implement to represent compressed liquid densities. Experimental densities for the system $\text{CO}_2 + \text{hexan-1-ol}$ are the first published as far as we could find in the literature. These data were successfully correlated using two different equations; however, the deviations obtained with the two correlations became larger as the CO_2 composition increase.

This is due to the system being more compressible, and these models cannot include this effect. The excess molar volumes were calculated in the whole range of reported data. These data were negative in the whole range of measurements and became more negative as the temperature increased at constant pressure meanwhile excess molar volumes became less negative as the pressure was increased at constant temperature.

Literature Cited

- (1) Saeki, T.; Hashimoto, K.; Fujishima, A.; Kimura, N.; Omata, K. Electrochemical reduction of CO₂ with high current density in a CO₂-methanol medium. *J. Phys. Chem.* **1995**, *99*, 8440–8446.
- (2) Wells, P. S.; Zhou, S.; Parcher, J. F. Unified chromatography with CO₂-based binary mobile phases. *Anal. Chem.* **2003**, *75*, 18A–24A.
- (3) Dooley, K. M.; Kao, C. P.; Gambrell, R. P.; Knopf, F. C. The use of entrainers in the supercritical extraction of soils contaminated with hazardous organics. *Ind. Eng. Chem. Res.* **1987**, *26*, 2058–2062.
- (4) Souvignet, I.; Olesik, S. V. Solvent-solvent and solute-solvent interactions in liquid methanol/carbon dioxide mixtures. *J. Phys. Chem.* **1995**, *99*, 16800–16803.
- (5) Nickel, D.; Schneider, G. M. Near-infrared spectroscopic investigations on phase behaviour and association of hexanol and 1-decanol in carbon dioxide, chlorotrifluoromethane, and sulfur hexafluoride. *J. Chem. Thermodyn.* **1989**, *21*, 293–305.
- (6) Lam, D. H.; Jangkamolkulchai, A.; Luks, K. D. Liquid-liquid-vapor phase equilibrium behavior of certain binary carbon dioxide + *n*-alkanol mixtures. *Fluid Phase Equilib.* **1990**, *60*, 131–141.
- (7) Gurdial, G. S.; Foster, N. R.; Yun, S. L. J.; Tilly, K. D. Phase behavior of supercritical fluid-entrainer systems. In *Supercritical Fluid Engineering Science: Fundamentals and Applications*; Kiran, E., Brennecke, J. F., Eds.; ACS Symposium Series 514; American Chemical Society: Washington, DC, 1993; pp 34–45.
- (8) Scheidgen, A. Fluidphasengleichgewichte Binärer und Ternärer Kohlendioxidmischungen mit Schwerflüchtigen Organischen Substanzen bis 100 MPa. Dissertation, Ruhr-Universität Bochum, Germany, 1997.
- (9) Chyliński, K.; Gregorowicz, J. Solubilities of (1-hexanol, or 1,2-hexanediol, or 2-hydroxypropanoic acid ethyl ester, or 2-hydroxyhexanoic acid ethyl ester) in supercritical CO₂. *J. Chem. Thermodyn.* **1998**, *30*, 1131–1140.
- (10) Gregorowicz, J.; Chyliński, K. On the solubility of chain alcohols in supercritical carbon dioxide. *Pol. J. Chem.* **1998**, *72*, 877–885.
- (11) Elizalde-Solis, O.; Galicia-Luna, L. A.; Sandler, S. I.; Sampayo-Hernández, J. G. Vapor-liquid equilibria and critical points of the CO₂ + 1-hexanol and CO₂ + 1-heptanol Systems. *Fluid Phase Equilib.* **2003**, *210*, 215–227.
- (12) Beier, A.; Kuranov, J.; Stephan, K.; Hasse, H. High-pressure phase equilibria of carbon dioxide + 1-hexanol at 303.15 and 313.15 K. *J. Chem. Eng. Data* **2003**, *48*, 1365–1367.
- (13) van Konynenburg, P. H.; Scott, R. L. Critical lines and phase equilibria in binary van der Waals mixtures. *Philos. Trans. R. Soc. London* **1980**, *298*, 495–540.
- (14) Stamoulis, D. Patterns of fluid phase behavior in binary and quasi-binary mixtures. Ph.D. Thesis, Delft University of Technology, Holland, 1994.
- (15) Roskar, V.; Dombro, R. A.; Prentice, G. A.; Westgate, C. R.; McHugh, M. A. Comparison of the dielectric behavior of mixtures of methanol with carbon dioxide and ethane in the mixture-critical region and liquid regions. *Fluid Phase Equilib.* **1992**, *77*, 241–259.
- (16) Galicia-Luna, L. A.; Richon, D.; Renon, H. New loading technique for a vibrating tube densimeter and measurements of liquid densities up to 39.5 MPa for binary and ternary mixtures of the carbon dioxide-methanol-propane system. *J. Chem. Eng. Data* **1994**, *39*, 424–431.
- (17) Galicia-Luna, L. A.; Richon, D.; Renon, H. Corrections: new loading technique for a vibrating tube densimeter and measurements of liquid densities up to 39.5 MPa for binary and ternary mixtures of the carbon dioxide-methanol-propane system. *J. Chem. Eng. Data* **1995**, *40*, 528–529.
- (18) Chang, C. J.; Day, C.-Y.; Ko, C.-M.; Chiu, K.-L. Densities and *P*-*x*-*y* diagrams for carbon dioxide dissolution in methanol, ethanol, and acetone mixtures. *Fluid Phase Equilib.* **1997**, *131*, 243–258.
- (19) Goldfarb, D. L.; Fernandez, D. P.; Corti, H. R. Dielectric and volumetric properties of supercritical carbon dioxide (1) + methanol (2) mixtures at 323.15 K. *Fluid Phase Equilib.* **1999**, *158-160*, 1011–1019.
- (20) Smith, R. L.; Lee, S. B.; Suzuki, S.; Saito, C.; Inomata, H.; Arai, K. Densities of carbon dioxide + methanol mixtures at temperatures from 313.2 to 323.2 K and at pressures from 10 to 20 MPa. *J. Chem. Eng. Data* **2002**, *47*, 608–612.
- (21) Pöhler, H.; Kiran, E. Volumetric properties of carbon dioxide + ethanol at high pressures. *J. Chem. Eng. Data* **1997**, *42*, 384–388.
- (22) Zúñiga-Moreno, A.; Galicia-Luna, L. A. Compressed liquid densities of carbon dioxide + ethanol mixtures at four compositions via a vibrating tube densimeter up to 363 K and 25 MPa. *J. Chem. Eng. Data* **2002**, *47*, 149–154.
- (23) Yaginuma, R.; Nakajima, T.; Tanaka, H.; Kato, M. Volumetric properties and vapor-liquid equilibria for the carbon dioxide + 1-propanol system at 313.15 K. *Fluid Phase Equilib.* **1998**, *144*, 203–210.
- (24) Zúñiga-Moreno, A.; Galicia-Luna, L. A.; Horstmann, S.; Ihmels, C.; Fischer, K. Compressed liquid densities and excess volumes for the binary systems carbon dioxide + 1-propanol and carbon dioxide + 2-propanol using a vibrating tube densimeter up to 25 MPa. *J. Chem. Eng. Data* **2002**, *47*, 1418–1424.
- (25) Yaginuma, R.; Nakajima, T.; Tanaka, H.; Kato, M. Densities of carbon dioxide + 2-propanol at 313.15 K and pressures up to 9.8 MPa. *J. Chem. Eng. Data* **1997**, *42*, 814–816.
- (26) Bridgman, P. W. The volume of eighteen liquids as a function of pressure and temperature. *Proc. Am. Acad. Arts Sci.* **1931**, *66*, 185–233.
- (27) Gylmanov, A. A.; Apaev, T. A.; Akhmedov, L. A.; Lipovetskii, S. I. Experimental study of the density of *n*-amyl and *n*-hexyl alcohols. *Izv. Vysh. Uchebn. Zaved. Neft Gaz* **1979**, *22* (7), 55–56 (in Russian).
- (28) Matsuo, S.; Makita, T. Volumetric properties of 1-alkanols at temperatures in the range 298–348 K and pressures up to 40 MPa. *Int. J. Thermophys.* **1989**, *10*, 885–897.
- (29) Uosaki, Y.; Kitaura, S.; Moryioshi, T. Compressions of 4-methyl-1,3-dioxolan-2-one and some alkanols at pressures up to 200 MPa and at the temperature 298.15 K. *J. Chem. Thermodyn.* **1992**, *24*, 559–560.
- (30) Shakhverdiev A. N.; Naziev Ya. M.; Safarov D. T. Thermal properties of various aliphatic alcohols near the line of phase-change liquid-vapor. *Zh. Prikl. Khim.* **1992**, *65*, 1631–1637.
- (31) Garg, S. K.; Banipal, T. S.; Ahluwalia, J. C. Densities, molar volumes, cubic expansion coefficients, and isothermal compressibilities of 1-alkanols from 323.15 to 373.15 K and at pressures up to 10 MPa. *J. Chem. Eng. Data* **1993**, *38*, 227–230.
- (32) Audonnet, F.; Pádua, A. A. H. Density and viscosity of mixtures of *n*-hexane and 1-hexanol from 303 to 423 K up to 50 MPa. *Int. J. Thermophys.* **2002**, *23*, 1537–1549.
- (33) Cibulka, I.; Zikova, M. Liquid densities at elevated pressures of 1-alkanols from C₁ to C₁₀: a critical evaluation of experimental data. *J. Chem. Eng. Data* **1994**, *39*, 876–886.
- (34) Starling, K. E. Thermo data refined for LPG, part 1: equation of state and computer prediction. *Hydrocarbon Process.* **1971**, *50*, 101–104.
- (35) Zúñiga-Moreno, A.; Galicia-Luna, L. A. Densities of 1-propanol and 2-propanol via a vibrating tube densimeter from 310 to 363 K and up to 25 MPa. *J. Chem. Eng. Data* **2002**, *47*, 155–160.
- (36) Wagner, W.; Pruss, A. The IAPWS formulation 1995 for the thermodynamic properties of ordinary water substance for general and scientific use. *J. Phys. Chem. Ref. Data* **2002**, *31*, 387–535.
- (37) Span, R.; Lemmon, E. W.; Jacobsen, R. T.; Wagner, W. A reference quality equation of state for nitrogen. *Int. J. Thermophys.* **1998**, *19*, 1121–1132.
- (38) Galicia-Luna, L. A.; Ortega-Rodríguez, A.; Richon, D. New apparatus for the fast determination of high-pressure vapor-liquid equilibria of mixtures and of accurate critical pressures. *J. Chem. Eng. Data* **2000**, *45*, 265–271.
- (39) Zúñiga-Moreno, A.; Galicia-Luna, L. A. Compressed liquid densities and excess volumes for the binary system CO₂ + *N,N*-dimethylformamide (DMF) from (313 to 363) K and pressures up to 25 MPa. *J. Chem. Eng. Data* **2005**, *50*, 1224–1233.
- (40) Zúñiga-Moreno, A.; Galicia-Luna, L. A.; Camacho-Camacho, L. E. Compressed liquid densities and excess volumes of CO₂ + decane mixtures from (313 to 363) K and pressures up to 25 MPa. *J. Chem. Eng. Data* **2005**, *50*, 1030–1037.
- (41) Zúñiga-Moreno, A.; Galicia-Luna, L. A.; Betancourt-Cárdenas, F. F. Compressed liquid densities and excess volumes of CO₂ + thiophene binary mixtures from 313 to 363 K and pressures up to 25 MPa. *Fluid Phase Equilib.* **2005**, *236*, 193–204.
- (42) Diaz-Peña, M.; Tardajos, G. Isothermal compressibilities of *n*-1-alcohols from methanol to 1-dodecanol at 298.15, 308.15, 318.15, and 333.15 K. *J. Chem. Thermodyn.* **1979**, *11*, 441–445.
- (43) Ortega, J. Densities and refractive indices of pure alcohols as a function of temperature. *J. Chem. Eng. Data* **1982**, *27*, 312–317.

- (44) Ortega, J. Densities and thermal expansivities of hexanol isomers at moderate temperatures. *J. Chem. Eng. Data* **1985**, *30*, 5–7.
- (45) Liew, K. Y.; Seng, C. E.; Ng, B. H. Viscosities of long chain *n*-alcohols from 15 to 80 °C. *J. Solution Chem.* **1993**, *21*, 1033–1040.
- (46) Rodriguez, M.; Galan, M.; Munoz, M. J.; Martin, R. Viscosity of triglycerides + alcohols from 278 to 313 K. *J. Chem. Eng. Data* **1994**, *39*, 102–105.
- (47) Hoyuelos, F. J.; Garcia, B.; Alcalde, R.; Ibeas, S.; Leal, J. M. Shear viscosities of binary mixtures of pyrrolidin-2-one with C₆–C₁₀ *n*-alkan-1-ols. *J. Chem. Soc., Faraday Trans.* **1996**, *92*, 219–225.
- (48) Lee, M.-J.; Lin, T.-K.; Pai, Y.-H.; Lin, K.-S. Density and viscosity for monoethanolamine + 1-propanol, + 1-hexanol, and + 1-octanol. *J. Chem. Eng. Data* **1997**, *42*, 854–857.
- (49) Span, R.; Wagner, W. A new equation of state for carbon dioxide covering the fluid region from the triple-point temperature to 1100 K at pressures up to 800 MPa. *J. Phys. Chem. Ref. Data* **1996**, *25*, 1509–1596.
- (50) Treszczanowicz, A. J.; Kiyohara, O.; Benson, G. C. Excess volumes for *n*-alkanols + *n*-alkanes, IV. Binary mixtures of decan-1-ol + *n*-pentane, + *n*-hexane, + *n*-octane, + *n*-decane, and + *n*-hexadecane. *J. Chem. Thermodyn.* **1981**, *13*, 253–260.

Received for review April 11, 2006. Accepted July 5, 2006. The authors thank CONACYT and IPN for their financial support.

JE060154F